

## DEVELOPMENT OF DESIGN OF AEROFOIL SHAPED FUSELAGE AND CFD INVESTIGATION OF ITS AERODYNAMIC CHARACTERISTICS

Wing Commander G.M. Jahangir Alam <sup>(1)</sup>, Dr. Md. Mamun <sup>(2)</sup>  
Dr. Md. Abu Taher Ali <sup>(3)</sup> and Dr. A. K. M. Sadrul Islam <sup>(4)</sup>

1. Department of Mechanical Engineering, Military Institute of Science & Engineering (MIST), Dhaka, Bangladesh, jahangiralam105@yahoo.com
- 2-3. Department of Mechanical Engineering, BUET, Dhaka, Bangladesh, mdmamun@me.buet.ac.bd & matali@me.buet.ac.bd
4. Department of Mechanical and Chemical Engineering, Islamic University of Technology (IUT), Gazipur, Bangladesh, sadrul@iut-dhaka.edu

### ABSTRACT

*This paper explains about the computational design procedure for designing of an Unmanned Air Vehicles (UAV) having "Aerofoil Shaped Fuselage". It also explains and analyses of the aerodynamic characteristics of an "Aerofoil Shaped Fuselage". This model could be used for designing of the future UAV which would be used for many military and civil applications like scientific data gathering, surveillance for law enforcement and homeland security, precision agriculture, forest fire monitoring, geological survey etc. NACA 4416 cambered aerofoil with chord length of 100 mm has been used for this computational design. The aerodynamic characteristics of Aerofoil Shaped Fuselage has been carried out at two different velocities (20 m/s & 40 m/s respectively) with different angles of attack from  $-3^\circ$  to  $18^\circ$  with  $3^\circ$  degree steps. This design has been made as well as numerical values have been obtained with the help of CFD software. The stalling angle for this design is found at about  $15^\circ$ . This model could be used for designing of the future UAV.*

**KEY WORDS:** Unmanned Air Vehicles (UAV), Aerofoil Shaped Fuselage, Aerodynamic Characteristics, Lift Coefficient, Drag Coefficient.

### 1.0 INTRODUCTION

An air vehicle having no onboard pilot and capable of pre-programmed operation as well as reception of intermittent commands either independently or from a human operator at a distance from the ground is called Unmanned Air Vehicle (UAV). The UAVs may operate independently or in cooperation with mother aircraft or ground bases sensors to carry out both military and civil applications. UAVs have been used to perform "dull, dirty and dangerous" missions successfully<sup>[1]</sup>. It can provide important information such as scientific data gathering, surveillance for law enforcement and homeland security, precision agriculture, forest fire monitoring, geological survey etc<sup>[2]</sup>.

UAVs mostly fly under low speed conditions. The aerodynamic characteristics of the UAVs have many similarities than that of the monoplane configuration. But UAV requires higher lifting force with a smaller size. In the recent years, the use of small UAVs for aerial surveillance in various civil applications has been increased manifold due to

greater deploy ability in comparison with the conventional manned aircraft. Due to the UAV's potential for carrying out so many tasks without direct risk to the crew or humans in general, they are ideal for testing new concepts which have been put forward as a means to further increase the vehicle's capability<sup>[3]</sup>.

This paper contains mainly the theoretical design and investigation of aerodynamic characteristics of a low speed UAV having "Aerofoil Shaped Fuselage" by using NACA 4416 profile with CFD software. The wings of a conventional UAV are producing the lift and its fuselage has very little or no contribution on producing lift. But UAV requires higher lifting force with a smaller size. As such, in order to maximize the efficiency of an UAV, it is assumed that the basic design of UAV could be changed and it should be such that all components of an UAV should contribute to the total lift. In such case, the concept of development of all lifting

vehicle technology would bring good result for research on design of future UAV. Hence, this paper will explain the development of the design of aerofoil shaped fuselage and analyze its flow pattern and aerodynamic characteristics at different angles of attack.

## 2.0 COMPUTATIONAL DESIGN

### 2.1 Important Features to be Considered for Computational Design

Important features for computational design are shown in Table 1.

**Table 1:** Important features of computational design.

| Nomenclature                 | Type  |
|------------------------------|---|
| Aerofoil                     | NACA 4416   |
| Flow of air                  | Incompressible and subsonic                       |
| Chord length of aerofoil     | 100 mm  |
| Air speed                    | 20 m/s and 40 m/s                                 |
| Density of air ( $\rho_0$ )  | 1.225 kg/m <sup>3</sup>                           |
| Operating pressure           | 1.01 bar  |
| Absolute viscosity ( $\mu$ ) | 1.789 x 10 <sup>-5</sup> kg/m-s                   |
| Reynold's Number (Re)        | 1.37 x 10 <sup>5</sup> and 2.74 x 10 <sup>5</sup> |
| Angles of attack             | -3° to 18° with 3° steps                          |
| Effect of temperature        | Neglected   |

### 2.2 Phases of Computational Design

CFD deals with the solution of fluid-dynamic equations on computers and the related use of computers in fluid-dynamics research<sup>[4]</sup>. There are three steps for designing an object successfully by using CFD software which are *Pre-processing*, *Computation* and *Post-processing* phases. The *pre-processing* phase consists of creation of geometry, meshing geometry, specify boundary type, set up the problem and solve.

Computation phase start with the import and scale of the mesh file designed at GAMBIT. In this phase, checking the grid of the physical model is to be carried out to ascertain the accuracy of design. On completion of entry of different data and setting up boundary conditions, the variables are to be initialized for convergent monitors. At the end, the designer is to go for feedback into the solver as well as for engineering analysis<sup>[5]</sup>. The typical solution

procedure overview to be followed during computation phase is shown in Figure 1.

To ascertain convergence result, each residual is to be reduced to a value of less than 10<sup>-3</sup>, except the energy residual, for which the default criterion is 10<sup>-6</sup>. Sometimes the residuals may not fall below the convergence criterion set in the case setup. However, by monitoring the representative low variables through iterations, it could be easily understood that the residuals have stagnated and do not change with further iterations. This could also be considered as convergence which usually seen for lift and drag coefficients. A sample of lift & drag coefficient indicating convergent criteria is shown in Figures 2 & 3 respectively.

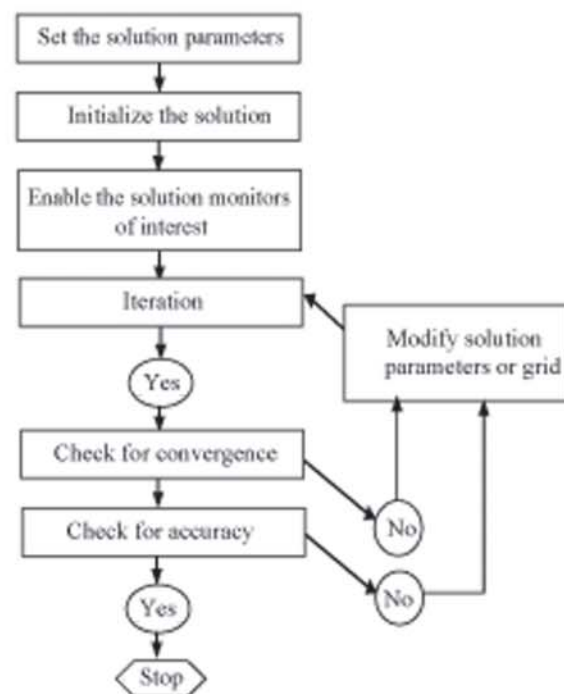


**Figure 1:** Typical Solution Procedure Overview.

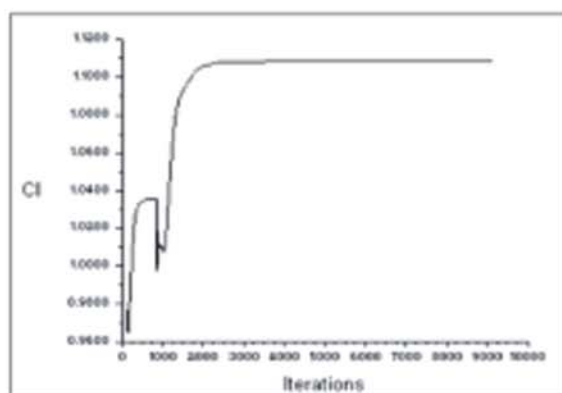


Figure 2: Lift Coefficient Plot.

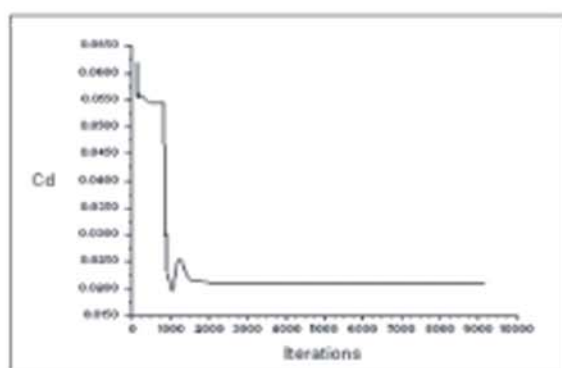


Figure 3: Drag Coefficient Plot.

At the post-processing phase, different engineering analyses have been carried out based on results, charts, graphs etc. The numerical results after engineering analyses would be used for experimental design, analysis of characteristics, manufacture of an object and detail investigation about an object.

### 3.0 CONFIGURATION LAYOUT

#### 3.1 Aerofoil Shaped Fuselage Model Design

Four major parts of the aerofoil shaped fuselage model are wing, fuselage, horizontal stabilizer and vertical stabilizer. Up wing type model has been selected. The total volume of the model is 534.102 cm<sup>3</sup>. The fuselage of this model is of aerofoil shaped like the wings. Important features which have been used during designing the wings and fuselages are shown in Table 2 and 3 respectively.

Table 2: Important features of wing.

| Nomenclature                                      | Type      |
|---|-----------|
| Aerofoil type                                     | NACA 4416 |
| Chord length of aerofoil                          | 100 mm    |
| Thickness of fuselage                             | 80 mm     |
| Tip to tip length of both wing                    | 480 mm    |
| Root to tip length of each wing (span)            | 200 mm    |
| Maximum thickness between upper and lower surface | 11.86 mm  |
| Nose Radius                                       | 2.48 mm   |
| Taper Angle                                       | Zero      |

Table 3: Important features of fuselage.

| Nomenclature                                      | Type      |
|---|-----------|
| Aerofoil type                                     | NACA 4416 |
| Chord length of aerofoil                          | 200 mm    |
| Tip to tip length of both fuselage                | 80 mm     |
| Root to tip length of each fuselage (span)        | 40 mm     |
| Maximum thickness between upper and lower surface | 23.70 mm  |
| Nose Radius                                       | 5 mm      |
| Taper Angle                                       | Zero      |

Total length, width and thickness of horizontal stabilizer are 140 mm, 30 mm and 4 mm respectively. It has been placed in a suitable position at the rear side of the fuselage. Total length, width and thickness of vertical stabilizer are 60 mm, 30 mm and 8 mm respectively. It has been also placed in a suitable position at the rear side of the fuselage. The wire-frame views of the aerofoil shaped fuselage model are shown in Figure 4.





Figure 6: Convergent Result of Aerofoil Shaped Fuselage Model.

#### 4.0 AERODYNAMIC CHARACTERISTICS

##### 4.1 Aerodynamic Characteristics of Aerofoil Shaped Fuselage Model at 20 m/s

The variation of lift coefficient with angle of attack at 20 m/s for aerofoil shaped fuselage model at different angle of attack is shown in Figure 7. The zero lift angle has been found at  $-3^\circ$  angle of attack. Then the lift coefficient increases almost linearly with the increase of angle of attack up to approximately  $15^\circ$ . In other words, the lift coefficient increases linearly with the increase of angle of attack up to  $15^\circ$ . After wards, the lift coefficient decreases with the further increase of angle of attack. As such, the stalling angle of proposed model is found at about  $15^\circ$ . It is also observed that the maximum lift coefficient,  $C_{l,max}$  for this type of model is approximately 1.20.

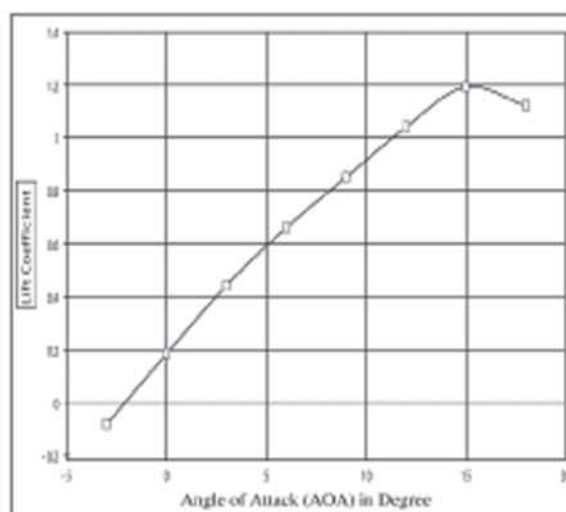
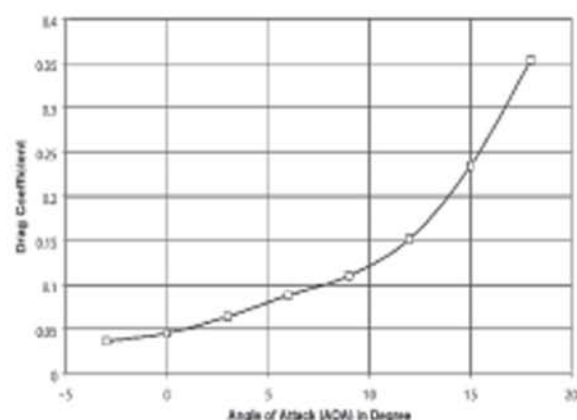


Figure 7: Variation of Lift Coefficient with Angle of Attack for Aerofoil Shaped Fuselage Model at 20 m/s [6].

The variation of drag coefficient with angle of attack at 20 m/s for aerofoil shaped fuselage model at different angle of attack is shown in Figure 8. The shape of the drag coefficient vs angle of attack curve is found exponential nature. As such, the drag coefficient increases with the increase of angle of attack. The value of drag coefficient for this proposed model at 15° angle of attack is found 0.234.



**Figure 8:** Variation of Drag Coefficient with Angle of Attack for Aerofoil Shaped Fuselage Model at 20 m/s [6].

#### 4.2 Aerodynamic Characteristics of Aerofoil Shaped Fuselage Model at 40 m/s

The variation of lift coefficient with angle of attack at 40 m/s for aerofoil shaped fuselage model at different angles of attack is shown in Figure 9. The zero lift angle has been found at -3° angle of attack. Then the lift coefficient increases almost linearly with the increase of angle of attack up to approximately 15°. In other words, the lift coefficient increases linearly with the increase of angle of attack up to 15°. After wards, the lift coefficient decreases with the further increase of angle of attack. As such, the stalling angle of aerofoil shaped fuselage model is found at about 15°. It is also observed that the maximum lift coefficient,  $C_{Lmax}$  of aerofoil shaped fuselage model is approximately 1.221.

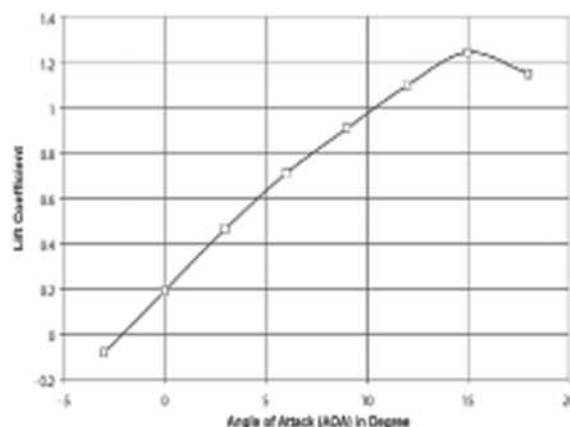


**Figure 9:** Variation of Lift Coefficient with Angle of Attack for Aerofoil Shaped Fuselage Model at 40 m/s [6].

The variation of drag coefficient with angle of attack at 40 m/s for aerofoil shaped fuselage model at different angle of attack is shown in Figure 10. The shape of the drag coefficient vs angle of attack curve is found exponential nature. As such, the drag coefficient increases with the increase of angle of attack. The value of drag coefficient for this model at 15° angle of attack is found 0.165.

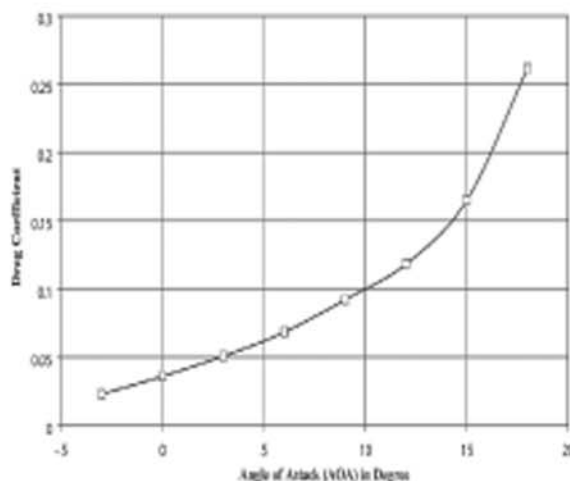


**Figure 10:** Variation of Drag Coefficient with Angle of Attack for Aerofoil Shaped Fuselage Model at 40 m/s [6].

#### 4.3 Flow of Air on Aerofoil Shaped Fuselage UAV Model

Air flows over the aerofoil shaped fuselage model at 20 m/s & 40 m/s respectively at different angles of attack from -3° to 18° with 3° increment. Stream line flow over the aerofoil sections of the wings as well

as flow separation from the trailing edge has been found during investigation. It is also seen that all components (surfaces) of the aerofoil shaped fuselage model contributed to the total lift. As such, this model is producing some extra lift from its fuselage along with its wing and this type of model might be a very better option to carry out research on designing future UAV model.

The aerofoil shaped fuselage model is producing extra drag due to increased fuselage frontal area, fuselage-wing interference effect and trailing edge vortex. The effect of fuselage frontal area is not that much significant here as the size of UAV is smaller. The fuselage-wing interference effect has also been reduced by selecting the up wing type model. More so, the concept of all body lifting structure would also open a good research arena for designing the future UAV. The visualization of air flow effect over this model is shown in Figure 11.

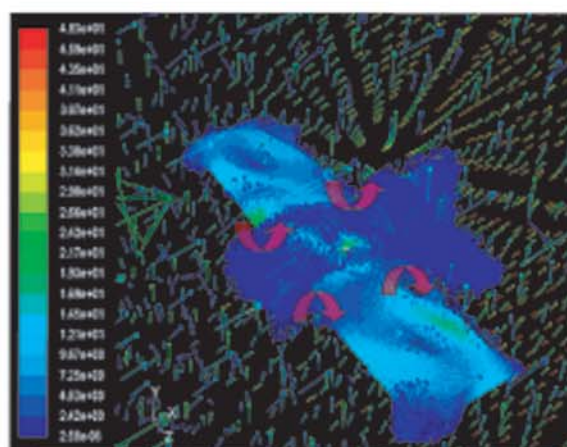


Figure 11: Flow of Air on Aerofoil Shaped Fuselage Model.

#### 4.4 Lift to Drag Ratio Curve of Aerofoil Shaped Fuselage Model

The lift drag ratio curve of aerofoil shaped fuselage at different velocities is shown in Figures 12. The lift to drag coefficient is found better for aerofoil shaped fuselage model having velocity 40 m/sec. From figure 10, it is found that both the lift and drag coefficient increase almost linearly up to stall angle of attack. Afterwards, a sharp increase of drag coefficient with reduction of lift coefficient occurs i.e. separation of flow starts after the stalling angle. Table 4 shows the lift to drag ratio curve at the stalling angle and two different velocities.

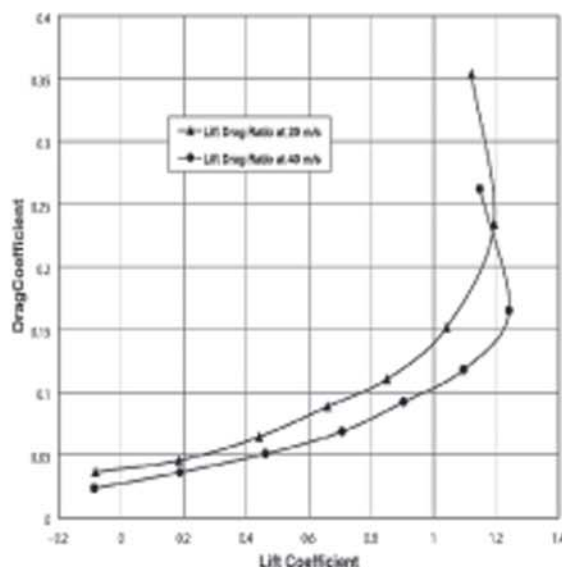


Figure 12: Comparison of Lift to Drag Ratio Curve of Aerofoil Shaped Fuselage Model at Different Velocities

Table 4: Lift Drag Ratio of Aerofoil Shaped Fuselage Configuration at the Stalling Angle and two Different Velocities (20 m/s & 40 m/s respectively).

| Configurations                           | Stall Angle | $C_{Lmax}$ | $C_{Dmax}$ | L/D Ratio |
|--|-------------|------------|------------|-----------|
| Aerofoil Shaped Fuselage Model at 20 m/s | 15.0°       | 1.20       | 0.234      | 5.13      |
| Aerofoil Shaped Fuselage Model at 40 m/s | 15.0°       | 1.221      | 0.165      | 7.40      |

#### 5.0 CONCLUSION

Operation of UAV proved to be easy and adaptable for versatile tasks including military as well as many civil applications in the recent years. But UAV requires higher lifting force with a smaller size. In order to maximize the efficiency of an UAV - the concept of development of all lifting vehicle technology might bring good result for research on designing future UAV. For this reason, the aerofoil shaped fuselage would be a good option for carrying out research in this field.

This paper explains the steps of computational design of a low speed aerofoil shaped fuselage model. NACA 4416 aerofoil profile and CFD

software have been used extensively for the design. The aerofoil shaped fuselage has produced a significant amount of extra lift from its fuselage due to its aerofoil shape. But this model has also produced some extra drag due to its increased fuselage frontal area, fuselage-wing interference effect and trailing edge vortex. The effect of fuselage frontal area is found minimum as the size of UAV is smaller. The fuselage-wing interference effect could also be reduced by selecting the up wing type model. However, research on ways for reduction of the trailing edge vortex from aerofoil shaped fuselage might be carried out afterwards for designing the future UAV.

## REFERENCES

- [1] Jodi A. Miller, Paul D. Minear, Albert F. Niessner, Jr, Anthony M. DeLullo, Brian R. Geiger, Lyle N. Long and Joseph F. Horn, "Intelligent Unmanned Air Vehicle Flight Systems", *Journal of Aerospace Computing, Information and Communication*, pp. 816-823, May 2007.
- [2] Randal Beard, Derek Kingston, Morgan Quigley, Deryl Snyder, Reed Christiansen, Walt Johnson, Timothy McLain and Michael A. Goodrich, "Autonomous Vehicle Technologies for Small Fixed-Wing UAVs", *Journal of Aerospace Computing, Information and Communication*, pp. 92-94, January 2005.
- [3] M. Secanell, A. Suleman and P. Gamboa "Design of a Morphing Airfoil for a Light Unmanned Aerial Vehicle using High-Fidelity Aerodynamic Shape Optimization" *Journal of American Institute of Aeronautics and Astronautics (AIAA 2005-1891)*, pp. 1-20, April 2005.
- [4] Jay P. Boris "New Directions in Computational Fluid Dynamics" *Annual Reviews*, pp 345-351, 1989.
- [5] Ramesh Agarwal "Computational Fluid Dynamics of Whole-Body Aircraft" *Annu. Rev. Fluid Mech.*, pp. 125-136, 1999.
- [6] G.M. Jahangir Alam, Dr. Md Mamun and Dr. A. K. M. Sadrul Islam, "Improved Aerodynamic Characteristics of Aerofoil Shaped Fuselage than that of the Conventional Cylindrical Shaped Fuselage", *International Journal of Scientific & Engineering Research*, Volume 4, Issue 1, January 2013.